Galvanomagnetic studies in γ-$Ni_{100-x-y}Fe_xCr_y$ permalloys ($5 \leqslant x \leqslant 23$; $2 \leqslant y \leqslant 21$)

S. Chakraborty and A. K. Majumdar*
Department of Physics, Indian Institute of Technology, Kanpur 208016, Uttar Pradesh, India
(Received 14 October 1997; revised manuscript received 20 January 1998)

High-resolution magnetoresistance data in both longitudinal and transverse orientations in some 15 different compositions of technologically important chrome permalloy γ-$Ni_{100-x-y}Fe_xCr_y$ ($5 \leqslant x \leqslant 23$; $2 \leqslant y \leqslant 21$) are presented at 4.2 K in magnetic inductions up to 14 kG along with Hall resistivity data for five Cr-rich alloys of composition $Ni_{75}Fe_{13}Cr_{12}$, $Ni_{70}Fe_{12}Cr_{18}$, $Ni_{75}Fe_5Cr_{20}$, $Ni_{72}Fe_8Cr_{20}$, and $Ni_{71}Fe_8Cr_{21}$. These are all ferromagnetic at 4.2 K. The maximum ferromagnetic anisotropy of resistivity (FAR) is found to be 0.76% for the alloy with the smallest Cr content (2 at. %). But as the Cr content increases, the FAR decreases drastically and becomes almost zero for the alloys with more than 18 at. % Cr. These results are discussed in terms of the split-band (SB) as well as the two-current conduction model. The experimental extraordinary Hall conductivity, $\gamma_{HS}=0$ line in the ternary phase diagram exhibits a pronounced curvature in the Cr-rich ($\simeq$ 20 at. %) region, contrary to the straight line predicted by the split-band model. But the most important observation is that the ridges of the constant FAR lines are found to follow exactly the experimental $\gamma_{HS}=0$ line. This behavior is in good agreement with the idea behind the SB model, but the experimental $\gamma_{HS}=0$ line and the line joining the ridges of the constant FAR lines deviate a lot from where they are theoretically predicted. The reason for such a discrepancy is attributed to the composition dependence of Z_{eff} that was taken as a constant in the SB model. Another possible reason is the uncertainty of the complete band splitting of Cr from those of Ni and Fe. However, a detailed theoretical investigation is needed to resolve it. Besides these, the small values of FAR in the present alloys could be ascribed to the large energy difference between the spin-up bands for Cr and Ni as shown by coherent potential approximation calculations. The decrease in the FAR with Cr can also be interpreted using the two-current conduction model. [S0163-1829(98)04830-9]

I. INTRODUCTION

The galvanomagnetic properties are considered to be the most important tools for knowing the electronic structure of metals and alloys, especially in ferromagnetic materials where spin-orbit interaction of $3d$ electrons is responsible for the low-field anisotropy of the galvanomagnetic data. Though it is an old problem, the interpretation still seems to be rather difficult and controversial. Recently, the problem was further compounded by structural and compositional disorders in concentrated alloys. In general, the longitudinal magnetoresistance (LMR) and the transverse magnetoresistance (TMR) of any conventional ferromagnet are positive and negative, respectively, at low fields. At higher fields, often called the technical saturation,[1] they show small changes. The ferromagnetic anisotropy of resistivity (FAR) is defined by

$$F=(\rho_{\parallel s}-\rho_{\perp s})/\rho^0=\Delta\rho_{\parallel s}/\rho^0-\Delta\rho_{\perp s}/\rho^0, \tag{1}$$

where F is the FAR, $\Delta\rho_{\parallel s}=\rho_{\parallel s}-\rho^0$, $\Delta\rho_{\perp s}=\rho_{\perp s}-\rho^0$, and ρ^0 is the zero-field ($H_{ext}=0$, where H_{ext} is the applied field) electrical resistivity. The values of $\Delta\rho_{\parallel s}/\rho^0$ and $\Delta\rho_{\parallel s}/\rho^0$ are obtained from the high-field LMR and TMR data extrapolated to zero internal magnetic field (H_{int}). The internal field H_{int} is defined as $H_{int}=H_{ext}-\beta M_s$ where β is the demagnetization factor that depends on the dimensions of the sample and its orientation with respect to the applied field, and M_s is the saturation magnetization. On the other hand, the Hall resistivity[1–3] in the case of ferromagnetic materials can be expressed as

$$\rho_H=R_0B_z+R_sM_s, \tag{2}$$

where R_0 is known as the ordinary Hall coefficient, B_z the magnetic induction inside the sample, and R_s the extraordinary Hall coefficient (EHC). R_0 is a manifestation of the Lorentz force acting on the conduction electrons whereas the origin of R_s is attributed to the spin-orbit interaction[2–4] present in a ferromagnet. In a flat Hall sample, the magnetic induction B_z inside the alloy ($B_z=\mu_0[H_{ext}+(1-\beta)M_s]$) is found to be the same as the applied induction μ_0H_{ext}, since the demagnetization factor β is almost equal to 1. The EHC, R_s shows temperature as well as impurity concentration dependence[2–4] through the relation

$$R_s\propto[\rho(C,T)]^n, \tag{3}$$

where $n=1$ represents the phenomenon of the skew scattering and $n=2$ the side-jump effect, and $\rho(C,T)$ is the electrical resistivity, which is a function of both impurity concentration (C) and temperature (T). The skew scattering ($R_s\propto\rho$), derived from the classical Boltzmann equation assuming a left-right asymmetry with respect to the plane containing the electron's spin and its momentum, is found to be predominant in pure metals or dilute alloys whereas the nonclassical side-jump effect ($R_s\propto\rho^2$) holds good in concentrated alloys. In describing the extraordinary Hall resistivity [R_sM_s, Eq. (2)] in concentrated ferromagnetic alloys (where contribution from the skew scattering is negligible), several authors[2–5] have suggested that $\gamma_{HS}(=R_sM_s/\rho^2)$, called the extraordinary Hall conductivity, is advantageous over R_sM_s in the sense that dividing by ρ^2, the concentration as well as

the temperature dependence of R_s gets eliminated. Hence γ_{HS} will have the same temperature dependence as that of M_s. However, the sign of γ_{HS} will remain the same as that of R_s. Here it is important to note that the FAR and γ_{HS} (i.e., the EHC) are inherent properties of a ferromagnet.[1]

In the last few decades, much work has been done experimentally[6–14] as well as theoretically[1,5,7,9,15–20] to understand FAR in Ni- and Fe-based alloys. Interestingly, most of the earlier studies[6–9,13] were focused on binary alloys with large FAR ($\simeq$10–20%). In an extensive study,[8] Van Elst had pointed out long back that adding a few atomic percent of Cr in Ni- and Fe-based alloys could decrease the value of FAR drastically. It is important to note that the value of the FAR is reported[8] as zero for 10.1 at. % Cr in $Ni_{100-x}Cr_x$ alloys. Since then, there is as such no detailed report on the FAR in Cr-rich alloys. On the other hand, the behavior of FAR in ternary alloy systems was found to be rather complicated and hence difficult to interpret. Later Berger and others[5,9,21,22] suggested that the split-band (SB) model could provide a satisfactory explanation for the composition dependence of FAR, EHC, and linear saturation magnetostriction in NiFeCu ternary alloys. The above SB model can also be applied to binary alloys. As a consequence, most of the earlier studies had dealt with binary alloys where the FAR was found to be very large (10–20 %). Till now, except for some scattered reports on amorphous alloys,[10,22] no detailed investigation on FAR along with EHC and linear magnetostriction coefficient (λ_s) has been made in any ternary crystalline systems suggested in the SB model except NiFeCu.

In this work, we have presented high-resolution magnetoresistance data in both longitudinal and transverse orientations on some 15 different compositions of chrome permalloy γ-$Ni_{100-x-y}Fe_xCr_y$ ($5 \leqslant x \leqslant 23$; $2 \leqslant y \leqslant 21$) at 4.2 K in magnetic inductions up to 14 kG. The values of the FAR are found to be much smaller than 0.1% for the high-Cr content (>12 at. %) alloys. Earlier, the change of sign of the EHC (Ref. 23) and the coefficient of the linear magnetostriction[24] (λ_s) (i.e., $R_S = \lambda_s = 0$) in the present alloy series could not be explained in terms of the split-band model. However, the study was restricted only to some low Cr-content alloys where their Curie temperatures (T_c) were found around and above room temperature. Here we have presented the Hall effect data on some Cr-rich alloys ($y \geqslant 18$) where the T_c's are below 77 K, and a relatively low Cr-content $Ni_{75}Fe_{13}Cr_{12}$ alloy with $T_c = 365$ K. The prime *motivation* behind the present investigation is to study the behavior of the FAR along with the extended $\gamma_{HS} = 0$ and the earlier reported $\lambda_s = 0$ lines in the ternary phase diagram of NiFeCr alloys with expected high initial permeability (μ). These will certainly provide some useful information regarding their electronic band structures. In addition, this will tell us whether the split-band model can provide a satisfactory explanation for such low-FAR alloys and also its general applicability. Besides these, we will try to explore possible reasons for such small FAR's in Cr-rich alloys. Further, the dc-magnetization study[25] on the present alloys had shown a transition from strong to weak itinerant ferromagnetism with increasing Cr. According to the two-current conduction model,[15,16] the above behavior should show up in the FAR data.

II. EXPERIMENTAL DETAILS

The alloys were prepared[26] by induction melting using ''Spec-pure'' grade of constituent materials. Then they were homogenized at 1100 °C for 48 h in an argon atmosphere. The bulk alloys were cold-rolled into thin strips from which samples of various shapes were cut for various measurements. Later they were annealed at 900 °C for 36 h and water quenched to keep their high-temperature γ (fcc) phase. The crystalline phase and the final composition have been checked thoroughly by x-ray and energy dispersive x-ray analysis, respectively.

Magnetoresistance and Hall-effect measurements have been made in a specially designed cryostat. The data acquisition is completely automated with a personal computer. A standard six-probe dc technique is used to measure both of them at a constant temperature of 4.2 K only. The currents used in the magnetoresistance and the Hall-effect measurements are 100 and 250 mA, respectively. The measurements are done in magnetic inductions up to 14 kG. The voltage and current leads are soldered to the samples with Zn-Cd nonsuperconducting solder. The relative accuracy in the magnetoresistance measurements is better than 1 part in 10^5. On the other hand, the Hall signal is found in the range of 1–3 μV with the misalignment voltage of less than 1 μV. Special care has been taken to reduce the noise level below 20 nV. The sign of the Hall voltage has been determined with respect to a standard Ni sample whose EHC is negative.

III. RESULTS AND DISCUSSION

The alloy designation, composition, Curie temperature (T_c), and resistivity value at 4.2 K ($\rho_{4.2\,K}$) are given in Table I. The values of T_c for almost all the alloys are taken from the earlier report on dc magnetization[25] except for S41, S47, and S50 where they are obtained from the recent ac-susceptibility measurements[27]. The typical behavior of the magnetoresistance ($\Delta\rho/\rho$) for low Cr-content ($x \leqslant 18$) and high Cr-content alloys ($x \geqslant 18$) are shown in Figs. 1 and 2, respectively. The plots for both longitudinal and transverse magnetoresistance for alloys S9, S26, S28, and S29 are given in Fig. 1 whereas those for S41 and S47 are presented in Fig. 2. In the low Cr-content alloys, the LMR is found to be positive while the TMR is negative. But in the high Cr-content alloys, both the LMR and the TMR are negative and nearly isotropic (see Fig. 2). Thus the FAR in the present alloys decreases with increasing Cr concentration. However, the isotropic nature of both the LMR and the TMR in the high Cr-content alloys is found to be quite puzzling although recently a similar behavior has been observed in Cr-rich $Fe_{80-x}Ni_xCr_{20}$ alloys.[28] The slopes $[(1/\rho)(d\rho/dH)]$ for both the LMR and the TMR data, beyond technical saturation, are coming positive in the low Cr-content alloys (see Fig. 1) whereas they are negative in the high Cr-content alloys. In conventional ferromagnets, a negative slope is generally expected that is explained in terms of both the reduced electron-magnon scattering as well as the slow increase in magnetization with applied field beyond saturation.[1] Earlier, a similar kind of positive magnetoresistance beyond technical saturation was observed in some Cr containing crystalline[8,11] and amorphous[11] alloys. This was described by the dominance of positive normal magnetoresistance[1]

TABLE I. Sample designation, alloy composition, ferromagnetic Curie temperature (T_c), value of resistivity ($\rho_{4.2\,K}$), FAR, extraordinary Hall resistivity (R_sM_s), and extraordinary Hall conductivity (γ_{HS}) at 4.2 K.

Alloy no.	Alloy compositions	T_c (K)	$\rho_{4.2\,K}$ ($\mu\Omega$ cm)	FAR (%)	R_sM_s (10^{-9} Ω m)	γ_{HS} (10^3 Ω^{-1} m^{-1})
S35	$Ni_{77}Fe_{21}Cr_2$	778 [a]	31	0.76	+0.9 [a]	+9.4
S9	$Ni_{85.5}Fe_{11}Cr_{3.5}$	620 [a]	40	0.38	−6.6 [a]	−41.3
S26	$Ni_{80}Fe_{16}Cr_4$	693 [a]	52	0.26	−1.5 [a]	−5.5
S32	$Ni_{69.5}Fe_{23}Cr_{7.5}$	635 [a]	60	0.16	+4.9 [a]	+13.6
S28	$Ni_{75}Fe_{17}Cr_8$	543 [a]	61	0.11	−1.9 [a]	−5.1
S29	$Ni_{75}Fe_{13}Cr_{12}$	365 [a]	82	0.05	−1.3	−1.9
S51	$Ni_{67}Fe_{21}Cr_{12}$	470 [a]	87	0.05	+5.9 [a]	+7.8
S33	$Ni_{68}Fe_{17.5}Cr_{14.5}$	320 [a]	88	0.04	+2.7 [a]	+3.5
S40	$Ni_{73.5}Fe_{11.5}Cr_{15}$	260 [a]	87	0.04	−2.9 [a]	−3.8
S42	$Ni_{78}Fe_6Cr_{16}$	185 [a]	85	0.07	−0.7 [a]	−1.0
S34	$Ni_{74}Fe_{12}Cr_{16}$	315 [a]	82	0.07	−0.7 [a]	−1.0
S48	$Ni_{70}Fe_{12}Cr_{18}$	179 [a]	78	0.02	+0.5	+0.8
S41	$Ni_{75}Fe_5Cr_{20}$	44	81	0.02	+0.3	+0.5
S50	$Ni_{72}Fe_8Cr_{20}$	60	84	0.00	+0.05	+0.1
S47	$Ni_{71}Fe_8Cr_{21}$	48	84	0.01	+0.2	+0.3

[a]Values taken from Ref. 23.

($\propto H^2$), arising due to the Lorentz force acting on the conduction electrons, over the negative ferromagnetic contribution. Very recently, a positive magnetoresistance[29] in Cr-rich $Cr_{100-x}Fe_x$ amorphous thin films was attributed to the strong spin-orbit interaction[30] in the weak localization limit. The present alloys are disordered with fairly large values of resistivity ($\rho_{4.2\,K} \simeq 31$–88 $\mu\Omega$ cm) (see Table I). The electrical resistivity study[27] on some of the present alloys has shown resistivity minima that are interpreted in terms of the electron-electron interaction effects in the weak localization limit.[31,32] Interestingly, both the electron-electron interaction effects and the weak localization in the presence of strong spin-orbit interaction give a positive magnetoresistance (H^2 in the low-field limit and $\sqrt{H}$ in the high-field limit), irrespective of their orientation. The present positive magnetoresistance in both longitudinal and transverse orientations is found to follow a similar H^2 dependence.[27] Moreover, the contribution of the normal magnetoresistance to the present data is calculated to be very small.[27] On the other hand, the recent ac-susceptibility study[27] in the Cr-rich alloys S41, S47, and S50 has shown a second magnetic phase transition at 9, 14, and 7 K, respectively, besides the ferromagnetic one at the respective Curie temperatures. According to the earlier neutron-diffraction and dc-magnetization study,[33] this low-temperature transition represents a spin-glass phase. The present magnetoresistance data are taken only at 4.2 K,

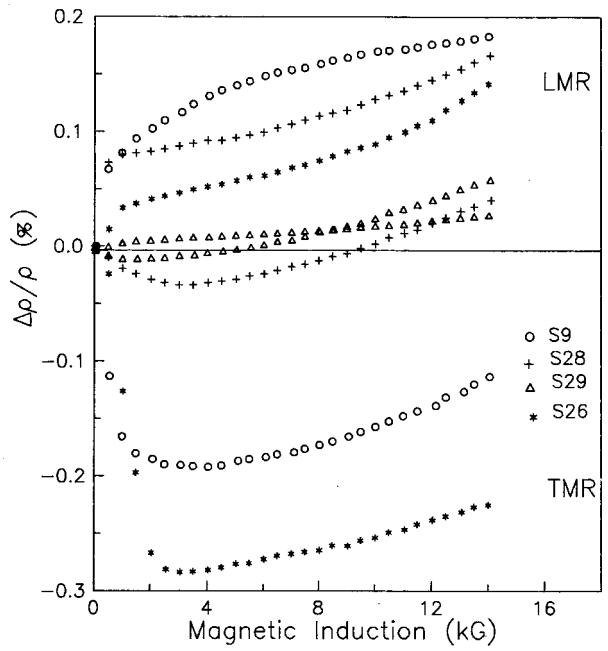

FIG. 1. Longitudinal (LMR) and transverse (TMR) magnetoresistance for alloys S9, S26, S28, and S29 at 4.2 K up to 14 kG of applied magnetic induction.

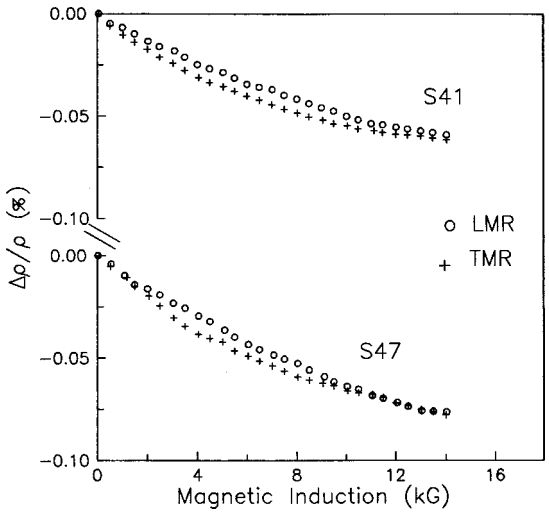

FIG. 2. Longitudinal (LMR) and transverse (TMR) magnetoresistance for alloys S41 and S47 at 4.2 K up to 14 kG of applied magnetic induction.

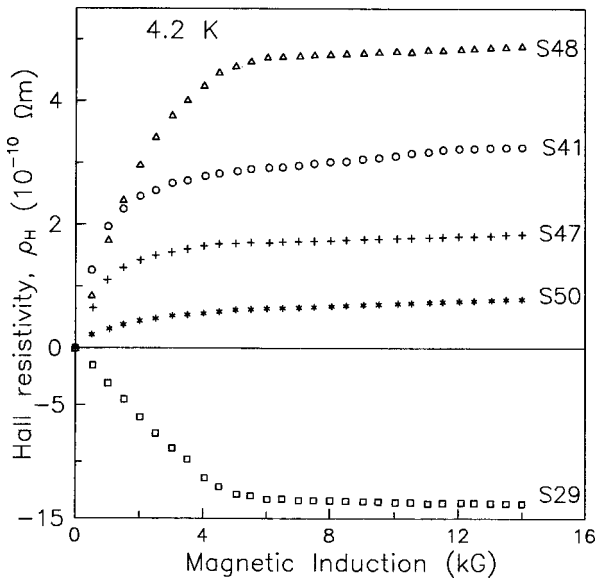

FIG. 3. Hall-resistivity (ρ_H) data for alloys S29, S41, S48, S47, and S50 at 4.2 K up to 14 kG of applied magnetic induction.

which is lower than the spin-glass transition temperatures. Hence a negative magnetic contribution arising from the spin-glass/cluster-glass phase[34] is quite expected, which can completely suppress the positive contribution. In addition, the isotropic behavior of both the LMR and the TMR provides a strong indication for the dominance of a spin-glass/cluster-glass contribution.[35] However, to say something more conclusively, one has to do the measurements at much higher fields[30] ($\simeq$10 T) and at lower temperatures ($\leqslant$ 1 K) that are not accessible to us.

The values of the FAR in all the alloys at 4.2 K are given in Table I. The maximum value of the demagnetization factor β is in the transverse direction and it is of the order of 2×10^{-2} and hence $\beta M_S \simeq 100$ Oe. The value of the zero-field electrical resistivity ρ^0 [see Eq. (1)] is obtained by averaging over directions of spontaneous magnetization, which for any cubic crystal can be written[11] as

$$\rho^0=\frac{1}{3}\rho_{\parallel s}+\frac{2}{3}\rho_{\perp s}=\rho+\frac{1}{3}\Delta\rho_{\parallel s}+\frac{2}{3}\Delta\rho_{\perp s}, \qquad (4)$$

where ρ is the electrical resistivity. A random distribution of domains, however, in these concentrated crystalline alloys is not obvious. Here, the values of $\rho_{4.2\,\mathrm{K}}$ are found to be much higher compared to those of $\Delta\rho_{\parallel s}$ and $\Delta\rho_{\perp s}$ (see Table I) and thus $\rho^0 \simeq \rho_{4.2\,\mathrm{K}}$.

The Hall resistivity (ρ_H) has been measured for the alloys S29, S41, S48, S47, and S50 at 4.2 K up to external magnetic inductions of 14 kG. The typical behavior of ρ_H for alloys S41, S48, S47, and S50 are shown in Fig. 3. The values of R_0 and R_sM_s are obtained from the slope and the intercept of the linear fit of the Hall-resistivity data beyond saturation. The signs of both R_0 and R_sM_s are positive for alloys S48, S41, S47, and S50 whereas they are negative for S29. The values of R_0 are found of the order of $(2–5)\times10^{-11}$ Ω mT^{-1} whereas those of R_sM_s are in the range of $(0.05–1.3)\times10^{-9}$ Ω m (see Table I). The absolute values of R_sM_s are found almost comparable with those of ρ_H since the values of R_0B_z (at 1 T) are more than two orders of magnitude smaller than those of R_sM_s. On the contrary, the electrical resistivity at 4.2 K is found to be almost three times greater than the Hall resistivity (see Table I). According to the side-jump effect,[2–4] this is quite expected in the present concentrated alloys (all the details are published elsewhere[36]). In Table I, the values of R_sM_s in the remaining alloys are taken from earlier reports.[23]

A. Description of FAR and γ_{HS} using the split-band model

Smit[7] and Van Elst[8] had shown long back that the FAR reaches a maximum of 20% in $Ni_{100-x}Fe_x$ and $Ni_{100-x}Co_x$ alloys with $x\simeq18$, which corresponds to almost the same 27.7 electrons per atom (e/a) ratio. Later on, extraordinary Hall[5,9,10,13,23] (R_s) and linear magnetostriction[21,22,24] (λ_s) coefficients were found to change their signs exactly at the same e/a ratio ($\simeq$27.7).[5,6] This seems to be in good agreement with the rigid band model.[8] But in ternary NiFeCu alloys, the above correlation does not hold, since the line $R_s\simeq\lambda_s\simeq0$ lies far away from the line of constant electron concentration. Berger had predicted earlier[5] that some orbital degeneracy exists in the $3d$ spin-down band near the Fermi level and the change of sign λ_s and R_s occurs when this orbital degeneracy crosses the Fermi level. Maximum FAR and initial permeability are also expected during this crossover. Later, Ashworth *et al.*[9] have extended this idea and proposed a model, called the SB model, for describing the changes of sign of R_s and λ_s in ternary NiFeM alloys (where M=Cr, V, Ti, W, Mo, etc.). According to the SB model, constituents of a given alloy have their own distinct $3d$ subbands separated from each other on the energy scale. This is possible only when the bands of all the constituents differ in energy by more than their average bandwidth.[13] The above condition is generally satisfied for concentrated alloys with valence difference (Z) between any two constituents greater than two, i.e., $Z\geqslant2$. In fact, the split-band model is found to be an extension of Friedel's virtual bound state (VBS) model.[37] The constituents of an alloy with the largest atomic number (i.e., nuclei most attractive to electrons) will have their subbands at the bottom while that with the smallest atomic number at the top. For NiFeM (where M=Cr, V, Ti, W, Mo, etc.) alloys, the bands for Ni are at the bottom whereas those of M are at the top (as shown in Fig. 4). In fact, there are some direct experimental evidences for such band splitting in NiCu alloys[39] from ultraviolet photoelectron spectroscopy and reflectivity measurements. The coherent potential approximation (CPA) calculations[40] for band structures in various Ni- and Fe-based alloys provide another strong theoretical support to the validity of the split-band model. Theoretical calculations illustrate that the composition variation of $R_s\simeq\lambda_s\simeq0$ is found to be associated with the zero expectation value of the Z component of the $3d$ orbital angular momentum[5,38] [$\langle L_z(E_F)\rangle=0$]. This happens when the Fermi energy (E_F) lies at the boundary or the gap between Fe $3d\downarrow$ and Ni $3d\downarrow$ bands. In other words, the EHC, R_s, and the linear magnetostriction coefficient λ_s change sign when the point T (where $3d$ spin-down bands of the Ni and Fe meet) crosses the Fermi level. According to Friedel's VBS model,[37] the total number of states in a given $3d$ subband is found to be equal to five times the atomic concentration of the respective constituent. The Fermi-level

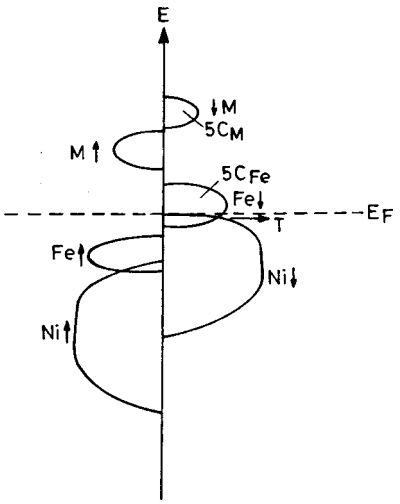

FIG. 4. Schematic band states for ternary Ni-Fe-M (M=Cr, V, etc.) alloys according to the split-band model.

crossover will occur when the total number of holes in the $3d$ band of the alloy is equal to the total number of the $3d\downarrow$ states of the Fe atom, i.e., for ternary NiFeM alloys, this condition can be written as

$$5C_{Fe}=0.55+2C_{Fe}-(10+Z)C_M,$$
$$3C_{Fe}+(10+Z)C_M=0.55, \tag{5}$$

where 0.55 is the number of holes per atom in Ni, C the atomic concentrations, and Z the valence difference between M and Ni (e.g., -4 for Cr, -5 for V, etc). The above equation [i.e., Eq. (5)] can also be applied to binary alloys. As, for example, in NiFe alloys, such a change of sign will occur when $3C_{Fe}=0.55$, i.e., around 18 at. % of Fe, which is consistent with the experimental results.[7,8] As a matter of fact, the above theory is found to be in good agreement with the experimental findings of the maximum value of the FAR and the change of sign of R_s and λ_s in Ni- and Fe-based binary alloys, and to some extent in ternary NiFeCu alloys. But, ironically, there is no detailed experimental study of FAR along with the location of $R_s=\lambda_s=0$ lines in any other ternary systems suggested in the split-band model.

The FAR is found to be much less than 1% in the present alloys. It is interesting to note that the alloys with high Cr content (i.e., 16 at. % or more) have almost zero FAR. This is consistent with the earlier data[8] by Van Elst. However, most of the studies, reported so far in support of the split-band model, have focussed on the alloys [NiFe, NiCo, NiFeCu (Ref. 9) (all are fcc), FeV, and FeCr (Ref. 13) (all are bcc)] where large FAR's (10–20 %) were observed. According to those, a maximum FAR ($\simeq$10–20 %) is expected when the point T of the $3d$ spin-down band of Ni approaches the Fermi level (Fig. 4). But this is not the case in the present γ-NiFeCr alloys. In the ternary phase diagram (i.e., in Fig. 5), the constant FAR lines are plotted using the present values. The FAR is found to decrease with increasing Cr concentration. The maximum FAR is found to be in the region where the alloy $Ni_{80}Fe_{20}$ lies. This is quite expected since the alloy γ-$Ni_{80}Fe_{20}$ has an FAR of 18%, the maximum value reported so far for any bulk crystalline alloy.[8] This certainly implies that the addition of Cr smears the orbital degeneracy

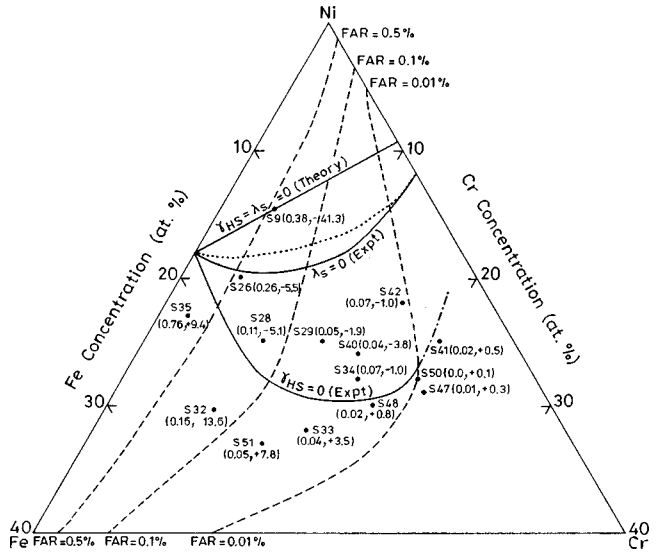

FIG. 5. Ternary phase diagram for Ni-Fe-Cr alloys. The alloys are represented by their sample designations. The numbers, given in the parentheses after the sample designations, are the values of the FAR (in %) and γ_{HS} (in units of $10^3\ \Omega^{-1}\ m^{-1}$), respectively. The dashed lines are contour lines for constant FAR. The experimentally obtained $\gamma_{HS}=0$ line (where the data for the solid line are taken from Ref. 23 and the dot-dashed line is the extended one; for details see Table I) is shown along with the theoretically predicted straight line (according to the split-band model [Eq. (5)]). The data for the experimental $\lambda_s=0$ (solid) line are taken from Ref. 24. For the dotted line, see text.

so that the average energy difference between the $3d$ branches in the vicinity of the Fermi level increases, which, in turn, destroys the FAR.

Coming back to the Hall-effect studies, the extended $\gamma_{HS}=0$ line is drawn on the ternary phase diagram (Fig. 5) of the present NiFeCr alloys using their positive and negative values along with the theoretical line, predicted by the SB model [Eq. (5)]. In Fig. 5, the alloys are represented by their sample designation (Table I). The two numbers in the parentheses, given after the sample designation, show the values of the FAR (in %) and γ_{HS} [in units of 10^3 $(\Omega\ cm)^{-1}$] at 4.2 K for the corresponding alloy. The experimental $\gamma_{HS}=0$ line is found to lie much below the theoretical line as it was observed in the earlier report.[23] The experimental line exhibits a curvature instead of a straight line as predicted by the SB model [Eq. (5)]. This curvature is found to be more pronounced in the high-Cr region of the phase diagram (Fig. 5). But the most important observation in the present study is that the ridges of the constant FAR lines are found to follow more or less exactly the experimental $\gamma_{HS}=0$ line in the direction of increasing Cr concentration. This is consistent with the idea behind the SB model, but the experimental $\gamma_{HS}=0$ line and the ridges of the constant FAR lines deviate a lot from where they are theoretically predicted. This is quite puzzling. In an earlier study,[24] the experimental $\lambda_s=0$ line (shown in Fig. 5) also exhibited a curvature in the ternary phase diagram for the present alloys. The probable reason for such a large deviation could be attributed to the concentration-dependent values of $(10+Z)$ (hereafter referred to as Z_{eff}) in Eq. (5) that is taken as a constant (for the

present NiFeCr alloys $Z_{eff}=6$) in the SB model. According to the Friedel's VBS model,[37] the average number of Bohr magneton per atom for the present alloys should follow a similar kind of relation with impurity concentration [i.e., M in the alloy NiFeM; Eq. (5)] and can be written as

$$\mu_{av}=\mu_{matrix}-(10+Z)C_M=0.55+2C_{Fe}-Z_{eff}C_M\,. \tag{6}$$

Earlier, the values of Z_{eff}, calculated from the dc-magnetization data,[25] were obtained in the range of 3.0–4.2, which is smaller than the expected value of 6. In addition, Z_{eff} is found to be highly concentration dependent. Substituting the values of Z_{eff} in Eq. (5), the modified theoretical line for $\lambda_s=R_s=0$ comes much closer to the experimental $\lambda_s=0$ line (still far away from the experimental $R_s=0$ line) with a small curvature in the Cr-rich region[23] [see dotted line in the ternary phase diagram (Fig. 5)]. In addition, an earlier neutron-diffraction study[41] had shown that the presence of Fe in Ni matrix (i.e., in NiFe alloy) does not influence the moment on the nearby Ni atoms. The moments at the Ni and the Fe sites are found to be 0.6 and (2.8 ± 0.2) (in units of Bohr magneton μ_B). On the other hand, Cr as impurity in Ni matrix introduces a large-spread magnetic moment disturbance[41] around Cr sites that is interpreted as an extended localized state in Ni alloys. The moment at the Cr site is found to be $(0.7\pm1.1)\mu_B$. Hence the bands for the present Cr-rich NiFeCr alloys are not so completely split as they are assumed to be in the SB model.[41] This can also be a plausible reason for such a large discrepancy between the experimental findings and the theoretical ones. Earlier studies in FeCr and FeV alloys[13] had pointed out a similar discrepancy, but not as large as it is in the present ternary alloys. Intensive theoretical as well as experimental investigations are needed to resolve it. Nevertheless, a complete study of FAR ($<1\%$) along with the corresponding $\gamma_{HS}=0$ and the earlier reported $\lambda_s=0$ lines is reported here for any ternary NiFe system. These compositions should lead to technologically important materials with very high initial permeability.

We now try to explore the possible reasons for such small values of FAR in the present γ-NiFeCr permalloys. It is very important to point out here that the addition of 2 at. % of Cr in Ni-Fe alloys reduces the FAR drastically almost from 18% [in $Ni_{80}Fe_{20}$) to 0.76% (in $Ni_{77}Fe_{21}Cr_2$ (S35)]. This is consistent with the earlier reported values[8] of 0.79% in $Ni_{99}Cr_1$. Very recently, this has also been found in amorphous alloys where the FAR decreases with increasing Cr concentration.[42,43] In Table I, the values of the FAR are listed where the maximum is found around 0.76% for S35 while the minimum is less than 0.01% for S50. It is to be noted here that the high resolution of the present data allows us to observe convincingly FAR of less than 0.1%. It is well known that the ferromagnetic anisotropy of resistivity is a manifestation of the spin-orbit interaction[9] and is usually expressed as

$$F=(A_{so}/\Delta E)^2+\cdots, \tag{7}$$

where the dots indicate higher-order terms, A_{so} is the spin-orbit parameter, and ΔE the energy difference between branches of the $3d$ band near the Fermi level. Earlier, the coherent potential approximation calculations[40] in $Ni_{90}Fe_{10}$ and $Ni_{90}Cr_{10}$ alloys have shown $(\Delta E)^{\downarrow}_{Fe-Ni}\simeq0.56$, $(\Delta E)^{\downarrow}_{Cr\text{-}Ni}\simeq0.52$, $(\Delta E)^{\uparrow}_{Fe-Ni}\simeq-0.06$, and $(\Delta E)^{\uparrow}_{Cr\text{-}Ni}\simeq0.7$ (all values are in units of half the bandwidth of the respective impurity). Here the signs $\downarrow$ and $\uparrow$ represent the spin-down and the spin-up bands, respectively. It is interesting to see that the FAR is almost unaffected by the energy difference between spin-down bands of FeNi and CrNi (where Fe and Cr are impurities in Ni matrix), since $(\Delta E)^{\downarrow}$ is almost the same in both the cases. On the contrary, the large energy difference in the spin-up bands for NiCr compared to that of NiFe is found to be mostly responsible for such low values of the FAR. $(\Delta E)^{\uparrow}_{Cr\text{-}Ni}$ is found to be an order of magnitude greater than $(\Delta E)^{\uparrow}_{Fe\text{-}Ni}$, which implies that addition of Cr in Ni matrix can effectively reduce the FAR by two orders of magnitude [see Eq. (7)]. This is in excellent agreement with the experimental values of 0.02% in the present S41 alloy ($Ni_{75}Fe_5Cr_{20}$) and the earlier observed values of 18% in $Ni_{80}Fe_{20}$ alloy. Hence, such small values of the FAR in the present γ-NiFeCr permalloys are quite understandable.

B. Description of FAR by the two-current conduction model

Campbell and co-workers had proposed a model, called the two-current conduction[15,16,18] (TCC), to describe the composition as well as the temperature dependence of FAR in binary and ternary Fe- and Ni-based alloys. The basic idea behind this model is that the $3d$ band of transition metals and alloys splits into spin-up and spin-down subbands due to the inherent ferromagnetic exchange interaction. As a result, the electrical conduction takes place in parallel through both spin-up and spin-down channels. The resistivity in each spin-up ($\rho_{\uparrow}$) and spin-down ($\rho_{\downarrow}$) channel has a series of contributions arising from s-s (ρ_{ss}) and s-d (ρ_{sd}) scattering of conduction electrons (i.e., s electrons). The residual resistivity, according to the TCC model, can be written as

$$\rho_0=\rho_{0\uparrow}\rho_{0\downarrow}/(\rho_{0\uparrow}+\rho_{0\downarrow}), \tag{8}$$

where $\rho_{0\uparrow}$ and $\rho_{0\downarrow}$ are the residual resistivity for spin-up and spin-down channels, respectively. In the absence of spin-orbit interaction, mixing of spin-up and spin-down states is not possible. In these circumstances, $\rho_{\uparrow}$ arises mainly from s-s scattering (ρ_{ss}) of like spin states (since there are no vacant $d\uparrow$ states at the Fermi level) while the contribution to $\rho\downarrow$ is coming from both s-s and s-d scattering of like-spin states. But in the presence of spin-orbit interaction, spin-up states acquire sufficient energy so that a certain amount of $d\uparrow$ characters can move into the $d\downarrow$ states at the Fermi level resulting in $d\uparrow$-$d\downarrow$ mixing. However, the transfer of $d\downarrow$ characters to $d\uparrow$ states is found to be highly anisotropic. The reason is that the magnetization direction induces a preferred axis for the spin-orbit coupling which, in turn, gives rise to resistivity anisotropy. After a rigorous calculation, the FAR in the low-temperature limit is expressed[15,16] as

$$F=\gamma[(\rho_{\downarrow}/\rho_{\uparrow})-1]=\gamma(\alpha-1), \tag{9}$$

where $\alpha=\rho_{\downarrow}/\rho_{\uparrow}$ and $\gamma(\simeq0.01)$ is a constant[16] independent of the scattering process. The TCC model is rather successful in explaining FAR in both crystalline[6,15,16] and amorphous[12] alloys. In strong ferromagnets[15,16] like NiFe and NiCu alloys[16], the calculated values of FAR are in very good agreement with experiments.

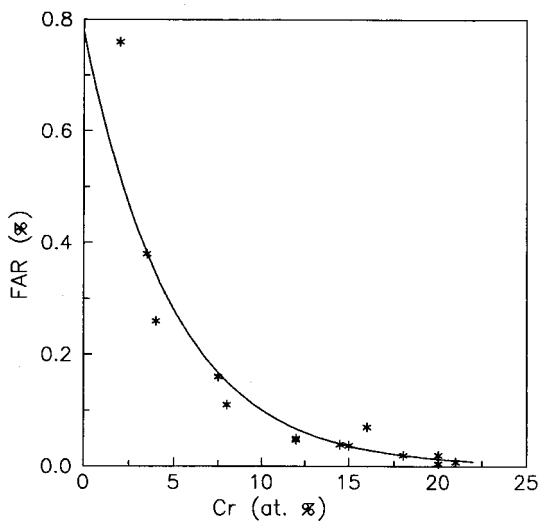

FIG. 6. Plot for the FAR against the Cr concentration (in at. %).

It is interesting to note here that Eq. (9) provides an important criterion for determining strong/weak itinerant-electron ferromagnetism in a given alloy. According to Stoner,[44] a strong ferromagnet is considered to have one subband (i.e., spin-up) completely full while in a weak ferromagnet both spin-up and spin-down subbands are partially filled. In strong ferromagnets, the conduction process takes place mostly through the spin-down subband, which implies that the contribution to resistivity comes mostly from $\rho_{\downarrow}$ (i.e., $\rho_{\downarrow} \gg \rho\uparrow$) resulting in $\alpha \gg 1$. Hence, a large FAR is expected in a strong ferromagnet. This is in good agreement with the large values of FAR in NiFe and NiCu. On the other hand, in a weak ferromagnet $\rho_{\uparrow}$ and $\rho_{\downarrow}$ are found to be almost comparable [i.e., $\alpha \simeq 1$) since both spin-up and spin-down subbands are available for conduction. As a result, its FAR will be very small [see Eq. (9)]. Earlier, Kaul and Rosenberg[12] employed the above idea in amorphous $(Fe\text{-}Ni)_{80}B_{20}$ and $(Fe\text{-}Ni)_{80}P_{14}B_{20}$ alloys to describe their ferromagnetic state. This, however, contradicts the earlier high-field magnetic data.[18,45] Later on, Malozemoff[18] proposed a modified TCC model for describing FAR in both amorphous and concentrated crystalline alloys. The dc-magnetization study[25] on the present alloy series has clearly shown a transition from strong to weak itinerant-electron ferromagnetism with increasing Cr concentration. In Table I, one can find that the FAR values exhibit a sharp decrease with increasing Cr content. The plot for the FAR with Cr concentration is shown in Fig. 6, where the FAR is found to fall almost exponentially and becomes nearly zero beyond $C_{Cr} \geqslant 12$ at. %. To get an estimate of $\rho_{\uparrow}$ and $\rho_{\downarrow}$, the expressions for them are derived[12] from Eqs. (8) and (9) as

$$\rho_{\downarrow} = \rho_0[\gamma^{-1}F + 2] \tag{10}$$

and

$$\rho_{\uparrow} = \rho_{\downarrow}[\gamma^{-1}F + 1]^{-1}. \tag{11}$$

The calculated values of $\rho_{\uparrow}$, $\rho_{\downarrow}$, and α for all the alloys at 4.2 K are shown in Table II. It is to be noted here that instead of ρ_0, $\rho_{4.2\,\mathrm{K}}$ is used in the above calculations since, according to the electrical resistivity study,[27], the values of ρ_0 and $\rho_{4.2\,\mathrm{K}}$ are found to be almost the same. However, the difference, if any, falls within the error limits of the measurements of the sample dimensions. In Table II, the value of $\rho_{\downarrow}$ is found to be two times greater than $\rho_{\uparrow}$ in low Cr-content alloys (e.g., S35). But as Cr concentration increases, they almost become comparable. It is very interesting to see that the value of α $(=\rho_{\downarrow}/\rho_{\uparrow})$ comes out to be almost one in Cr-rich alloys ($C_{Cr} \geqslant 12$). This clearly indicates that with increasing Cr concentration the present NiFeCr alloys moves towards weak itinerant ferromagnetism in good agreement with the dc-magnetization study.[25] To our knowledge, this is probably the first time when the magnetic state of a crystalline Cr-rich ternary alloy series is correlated with the FAR using the TCC model.

TABLE II. Sample designation, alloy composition, values of resistivity for spin-down ($\rho_{\downarrow}$) and spin-up ($\rho_{\uparrow}$) bands at 4.2 K, and their ratio α $(\rho_{\downarrow}/\rho_{\uparrow})$.

Alloy no.	Alloy compositions	$\rho_{\downarrow}$ (4.2 K) ($\mu\Omega$ cm)	$\rho_{\uparrow}$ (4.2 K) ($\mu\Omega$ cm)	α $(=\rho_{\downarrow}/\rho_{\uparrow})$
S35	$Ni_{77}Fe_{21}Cr_2$	86	49	1.77
S9	$Ni_{85.5}Fe_{11}Cr_{3.5}$	95	69	1.38
S26	$Ni_{80}Fe_{16}Cr_4$	118	93	1.26
S32	$Ni_{69.5}Fe_{23}Cr_{7.5}$	130	112	1.16
S28	$Ni_{75}Fe_{17}Cr_8$	129	116	1.11
S29	$Ni_{75}Fe_{13}Cr_{12}$	174	166	1.05
S51	$Ni_{67}Fe_{21}Cr_{12}$	178	169	1.05
S33	$Ni_{68}Fe_{17.5}Cr_{14.5}$	180	173	1.04
S40	$Ni_{73.5}Fe_{11.5}Cr_{15}$	178	171	1.04
S42	$Ni_{78}Fe_6Cr_{16}$	176	166	1.07
S34	$Ni_{74}Fe_{12}Cr_{16}$	170	159	1.07
S48	$Ni_{70}Fe_{12}Cr_{18}$	158	155	1.02
S41	$Ni_{75}Fe_5Cr_{20}$	164	161	1.02
S50	$Ni_{72}Fe_8Cr_{20}$	168	168	1.00
S47	$Ni_{71}Fe_8Cr_{21}$	169	167	1.01

IV. CONCLUSION

In conclusion, high-resolution magnetoresistance data in both longitudinal and transverse orientations in some 15 different compositions of chrome permalloy γ-$Ni_{100-x-y}Fe_xCr_y$ $(5 \leqslant x \leqslant 23;\ 2 \leqslant y \leqslant 21)$ are presented at 4.2 K in magnetic inductions up to 14 kG along with Hall-resistivity data for five of them (S29, S41, S48, S47, and S50). The FAR values are found to be very small in the present NiFeCr alloys. A maximum value of 0.76% is found in the alloy S35 with 2 at. % of Cr. But as the Cr content increases, the value of the FAR decreases drastically and for S50 ($Ni_{72}Fe_8Cr_{20}$) it becomes almost zero. This is consistent with the earlier reported values[8] for $x \geqslant 10$ at. % in $Ni_{100-x}Cr_x$ alloy. The experimental $\gamma_{HS} = 0$ line is shown in the ternary phase diagram (Fig. 5). It is found to deviate strongly from the theoretical line. In addition, the experimental line has shown a pronounced curvature in the Cr-rich ($\simeq 20$ at. %) region in contrast to the straight line predicted by the split-band model [Eq. (5)]. But the most *important* observation is that the ridges of the constant FAR lines are found to follow exactly the experimental $\gamma_{HS} = 0$ line. Also, the initial permeability (μ) for these compositions should be

very high making them useful as transformer core materials. All these are in good agreement with the idea behind the SB model. However, the experimental $\gamma_{HS}=0$ line and the line joining the ridges of the constant FAR lines are found to lie far away from where they are theoretically expected. This is quite puzzling. One of the reasons for such a discrepancy is in the composition dependence of Z_{eff} that was taken to be a constant in the split-band model. According to earlier studies, a complete band splitting, as predicted by the SB model, is quite unexpected for the present Cr-rich alloys and this might also be another reason for the discrepancy. Nevertheless, the present work provides values of the FAR for high Cr-content alloys. The large energy difference between the spin-up bands of Cr and Ni (as found from CPA calculations) is responsible for such small values of the FAR in these high Cr-content alloys. In addition, according to the two-current conduction model, the decrease in the FAR values with increasing Cr is interpreted in terms of the alloys moving from strong to weak itinerant ferromagnetism. This conclusion is in excellent agreement with the earlier dc-magnetization data of the present alloys.[25]

ACKNOWLEDGMENTS

We are grateful to the Department of Science and Technology, Government of India, for providing financial support through Project No. SP/S2/M-24/93. Also financial assistance from NSF Grant No. INT-9602975 is gratefully acknowledged.

*Author to whom correspondence should be addressed. Electronic address: akm@iitk.ernet.in

[1] J.P. Jan, in *Solid State Physics*, edited by F. Seitz and D. Turnbull (Academic, New York, 1957), Vol. 5, p. 1.
[2] L. Berger and G. Bergmann, in *The Hall Effect and its Applications*, edited by C.L. Chien and C.R. Westgate (Plenum, New York, 1980), p. 55.
[3] T.R. McGuire, R.J. Gambino, and R.C. O'Handley, in *The Hall Effect and Its Applications* (Ref. 2), p. 137.
[4] L. Berger, Phys. Rev. B **2**, 4559 (1970).
[5] L. Berger, Physica (Amsterdam) **30**, 1141 (1964).
[6] T.R. Macguire and R.I. Potter, IEEE Trans. Magn. **MAG-11**, 1018 (1975).
[7] J. Smit, Physica (Amsterdam) **16**, 612 (1951).
[8] H.C. Van Elst, Physica (Amsterdam) **25**, 708 (1959).
[9] H. Ashworth, D. Sengupta, G. Schnakenberg, L. Shapiro, and L. Berger, Phys. Rev. **185**, 172 (1969).
[10] R.C. O'Handley, Phys. Rev. B **18**, 2577 (1978).
[11] A.K. Nigam and A.K. Majumdar, Physica B & C **95**, 385 (1978).
[12] S.N. Kaul and M. Rosenberg, Phys. Rev. B **27**, 5698 (1983).
[13] L. Berger, in *Magnetism and Magnetic Materials*, edited by J.J. Becker and G.H. Lander, AIP Conf. Proc. No. 34 (AIP, New York, 1976), p. 355.
[14] H. Ma, Z. Wang, H.P. Kunkel, and Gwyn Williams, J. Phys. C **4**, 1993 (1992).
[15] I.A. Campbell, A. Fert, and O. Joul, J. Phys. C **3**, S95 (1970).
[16] I.A. Campbell, A. Fert, and O. Joul, J. Magn. Magn. Mater. **5**, 23 (1977); J. Phys. F **6**, 849 (1976).
[17] J. Banhart and H. Ebert, Europhys. Lett. **32**, 517 (1995).
[18] A.P. Malozemoff, Phys. Rev. B **32**, 6080 (1985).
[19] L. Berger, P.P. Freitas, J.D. Warner, and J.E. Schmidt, J. Appl. Phys. **64**, 5459 (1988).
[20] L. Berger, J. Appl. Phys. **67**, 5549 (1990).
[21] L. Berger, Phys. Rev. **138**, A1083 (1965).
[22] R.C. O'Handley, Phys. Rev. B **18**, 930 (1978); R.C. O'Handley and L. Berger, in *Proceedings of the International Conference on the Physics of Transition Metals, Toronto*, edited by M. J. G. Lee, J. M. Perz, and E. Faucett, IOP Conf. Proc. No. 39 (Institute of Physics, London, 1978), Chap. 6, p. 477.
[23] A.K. Gangyopadhyay, R.K. Ray, and A.K. Majumdar, Phys. Rev. B **30**, 1801 (1984).
[24] A.K. Majumdar and R.D. Greenough, J. Magn. Magn. Mater. **59**, 57 (1986).
[25] A.K. Gangyopadhyay, R.K. Ray, and A.K. Majumdar, Phys. Rev. B **30**, 6693 (1984).
[26] Anup Kumar Gangyopadhyay, Ph.D. thesis, Indian Institute of Technology, Kanpur, India, 1983.
[27] S. Chakraborty and A.K. Majumdar, J. Magn. Magn. Mater. **186**, 357 (1998).
[28] S. Banerjee and A.K. Roychoudhury, Phys. Rev. B **52**, 3453 (1995); T.K. Nath and A.K. Majumdar, J. Appl. Phys. **70**, 5828 (1991).
[29] Y. Özdemir, A. Kilic, M. Özdemir, H. Celik, and S. Senoussi, J. Phys. C **8**, 11 121 (1996).
[30] J.B. Bieri, A. Fert, G. Creuzet, and A. Schuhl, J. Phys. F **16**, 2009 (1986).
[31] B.L. Ałtshuler, A.G. Aronov, A.I. Larkin, and D. Khmel'nitskii, Zh. Éksp. Teor. Fiz. **81**, 768 (1981) [Sov. Phys. JETP **54**, 411 (1981)].
[32] P. A. Lee and T. V. Ramakrishnan, Rev. Mod. Phys. **57**, 287 (1985).
[33] A.Z. Menshikov, G.A. Takzey, and A.Ye. Teplylykh, Phys. Met. Metallogr. **54**, 41 (1982); A.K. Majumdar and P.V. Blanckenhagen, Phys. Rev. B **29**, 4079 (1984).
[34] M.T. Béal-Monod and R.A. Weiner, Phys. Rev. **170**, 552 (1968); Abhijit Mookerjee, J. Phys. F **10**, 1559 (1980).
[35] A.K. Nigam and A.K. Majumdar, Phys. Rev. B **27**, 495 (1983).
[36] S. Chakraborty and A.K. Majumdar, Phys. Rev. B **57**, 11 850 (1998).
[37] J. Friedel, Nuovo Cimento **7**, 287 (1958).
[38] L. Berger, Physica **91**B, 31 (1977).
[39] B. Velicky, S. Kirkpattrick, and H. Ehrenreich, Phys. Rev. **175**, 747 (1968).
[40] Hideo Hasegawa and Junjiro Kanamori, J. Phys. Soc. Jpn. **33**, 1599 (1972); **33**, 1607 (1972).
[41] M.F. Collins and G.G. Low, Proc. Phys. Soc. London **86**, 535 (1965).
[42] A. Das and A.K. Majumdar, J. Appl. Phys. **70**, 6323 (1991).
[43] R. Kern, M. Naka, U. Gonsor, H. Fujimori, and I. Okamoto, J. Magn. Magn. Mater. **31-34**, 1471 (1983).
[44] E.C. Stoner, Proc. R. Soc. London, Ser. A **165**, 372 (1938).
[45] R.C. O'Handley and D.S. Boudreau, Phys. Status Solidi A **45**, 607 (1978).